Article

Catalyst Loading Controls Chemoselectivity: Unusual Effect in Rhodium(II) Carbene Insertion Reactions with Tetrahydrofuran [†]

Alexander Kazantsev [1], Ivan A. Rodionov [1], Olga Bakulina [1], Grigory Kantin [1], Dmitry Dar'in [1,*] and Mikhail Krasavin [1,2,*]

1   Institute of Chemistry, Saint Petersburg State University, 199034 St. Petersburg, Russia
2   Institute for Medicine and Life Sciences, Immanuel Kant Baltic Federal University, 236041 Kaliningrad, Russia
*   Correspondence: d.dariin@spbu.ru (D.D.); m.krasavin@spbu.ru (M.K.)
†   This article is dedicated to the upcoming 300th Anniversary of Saint Petersburg University.

Abstract: *(E)*-3-Arylidene-4-diazopyrrolidine-2,5-diones previously shown to yield two products in reactions with tetrahydrofuran mediated by rhodium carbenes—tetrahydrofur-2-yl-substituted product of C-H insertion and spirocyclic product of formal C-O insertion. Accidentally, it was noted that the ratio of the two products depends on the catalyst loading, and the phenomenon was investigated in detail. It was found to be of preparative significance: by solely changing the catalyst loading from 0.01 mol% to 10 mol%, one can obtain sound yields of either of the two products. Mechanistic and kinetic interpretation of this new phenomenon has been proposed.

Keywords: α-diazocarbonyl compounds; diazo succinimides; rhodium catalyst; rhodium carbenes; C-H insertion; C-O insertion; catalyst loading

1. Introduction

Metal carbene species generated from α-diazocarbonyl compounds can display a number of useful reactivities [1]. Among these, insertion into heteroatom-hydrogen [2], carbon-hydrogen [3], and carbon-heteroatom [4] bonds as well as various ring-forming processes—e.g., [2 + 1] cycloaddition to double carbon-carbon and carbon-oxygen bonds resulting in the formation of cyclopropanes [5] and oxiranes [6], respectively, as well as [3 + 2] cycloaddition with nitriles delivering oxazoles [7] are perhaps the most notable. However, when a particular substrate can react with carbonyl-substituted metal carbenes in more than one competing way, the issue of chemoselectivity and the prospect of directing the process toward only one desired product among several possible becomes quite pressing.

In 2020 we reported a facile, Rh(II)-catalyzed spirocyclization of *(E)*-3-arylidene-4-diazopyrrolidine-2,5-diones **1** (α-diazo arylidene succinimides or DAS) with tetrahydrofuran leading to spirocyclic perhydropyrans **2** [8]. The process is thought to involve the formation of an oxonium ylide species (vide infra) followed by a Stevens-type rearrangement resulting in the [n+1] ring expanded product **2**. However, the formation of the latter, possessing an intriguing and rather unique spirocyclic framework, was accompanied by C-H insertion of the rhodium(II) carbene to tetrahydrofuran and the formation of a substantial amount of tetrahydrofuryl-substituted succinimides **3** as a diastereomeric mixture (Scheme 1). This was certainly viewed as an obstacle to considering the method to be of significant preparative value as neither spirocycle **2** nor succinimide **3** were the sole product, and the two had to be separated by tedious chromatography in order to obtain them as individual products. However, metal-catalyzed synthetic transformations of DAS are of significant preparative value for the rapid generation of molecular complexity [9–12]. Thus, improving the yield of the reaction depicted in Scheme 1 toward a specific product was highly desirable.
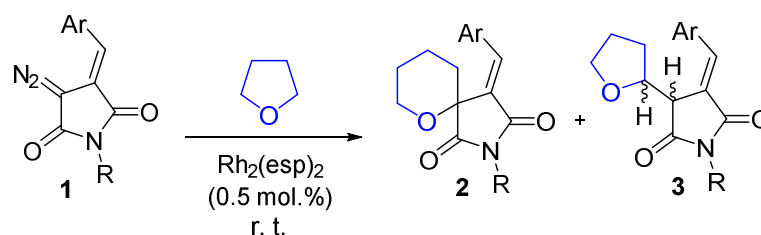
Scheme 1. Rh(II)-catalyzed reaction of *(E)*-3-arylidene-4-diazopyrrolidine-2,5-diones **1** with tetrahydrofuran.

We continued studying this reaction and soon discovered, somewhat by accident, that using a 10-fold lower amount of the catalyst, a significantly higher proportion of the valuable spirocyclic product **2** could be obtained (although the substrate conversion was markedly slower). Intrigued by this phenomenon, we set off to investigate it in more detail and perhaps gain a mechanistic understanding of the observed shift in chemoselectivity. Herein, we present the results obtained in the course of this investigation.

2. Results and Discussion

As the model substrate for studying the chemoselectivity shift phenomenon described above, we selected compound **1a** (Ar = Ph, R = Bn), which we deemed highly suitable for the following reasons. The substituents around the DAS core are electron-neutral, which excludes possible bias due to substituents' effects; the yields we obtained earlier for products **2a** and **3a** were nearly equal (40% and 42%, respectively) [8], which makes it convenient to observe the chemoselectivity shift on alteration of the catalyst loading.

First, we became interested in monitoring the HPLC yield of products **2a** and **3a** at different time points (see Figure 1 for a typical chromatogram of the reaction mixture). The amount of Rh$_2$(esp)$_2$ catalyst was reduced five-fold compared to the protocol described earlier [8] in order to slow the reaction down and allow for the HPLC monitoring of it with a gradually increasing degree of conversion (with 0.5 mol% of the catalyst the reaction was too fast). As follows from the data summarized in Table 1, the full conversion was achieved in 6 h. At the same time, the ratio **3a:2a** (expressed as % fraction of **3a** in the total product yield) remained virtually unchanged over the course of the reaction.
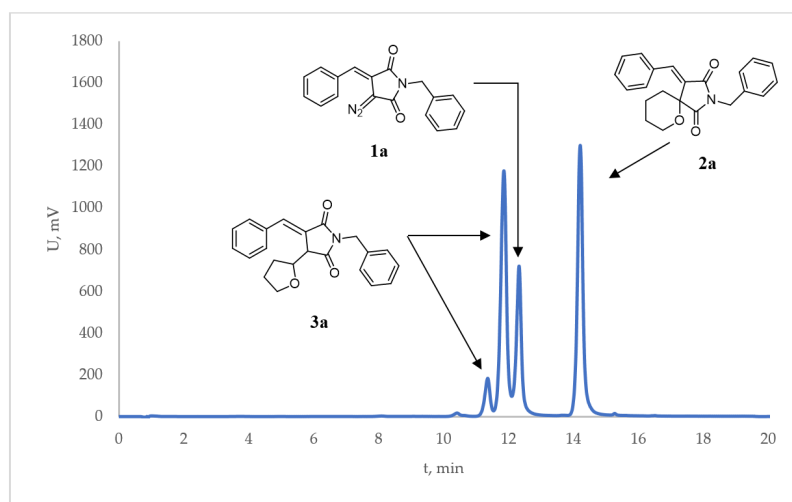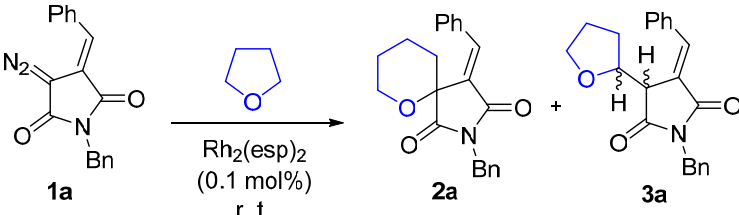

Figure 1. Typical HPLC chromatogram of a mixture consisting of **1a**, **2a,** and **3a** components (**3a** was formed as a mixture of diastereomers).

Table 1. Results of HPLC monitoring of reaction **1a** → **2a** + **3a**.

Time, min	Conversion (%)	Yield of 2a (%)	Yield of 3a (%)	Ratio 2a:3a
2	2	2	1	69:31
15	16	10	5	67:33
30	29	23	11	68:32
45	41	27	13	67:33
60	51	34	16	66:34
90	67	39	21	65:35
120	76	47	24	66:34
150	84	50	25	65:35
180	89	52	27	66:34
240	95	55	29	65:35
300	98	57	30	65:35
360	100	59	32	64:36

The composition of **1a** → **2a** + **3a** reaction mixture monitored over 6 h can be graphically presented, as shown in Figure 2. The observed composition, indeed, can be interpreted as the result of competing reaction pathways rather than the potential interconversion of products **2a** and **3a**. In a control experiment, product **3a** was kept in THF in the presence of Rh$_2$(esp)$_2$ catalyst (1 mol%) at 30 °C for up to seven days, whereupon it remained completely unchanged (i.e., no product **2a** was observed).
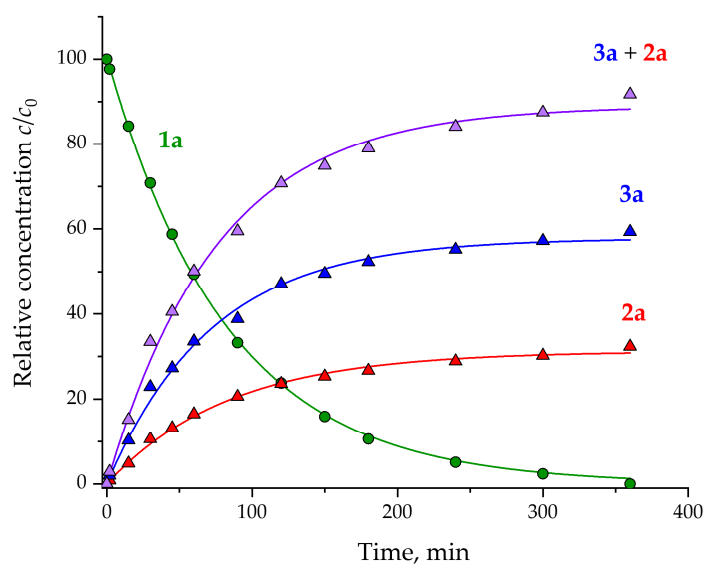
Figure 2. The changes in the composition of **1a** → **2a** + **3a** reaction mixture up to full conversion (green for **1a**, red for **2a**, blue for **3a** and purple for **2a** + **3a**).

The kinetic curve of the disappearance of diazo compound **1a** is well approximated by an exponential equation $c = c_0\exp(-kt)$, which corresponds to a pseudo-first-order

reaction with a rate constant $k = (12.1 \pm 0.1) \times 10^{-3}$ min^{-1}. The curves corresponding to the accumulation of products **2a** and **3a** are also approximated by a pseudo-first-order kinetic equation $c = c_{\infty}(1 - \exp(-kt))$. The total product yield (**2a** + **3a**) was 92% which is likely due to the unidentified side reactions or decomposition of diazo compound **1a** under the reaction conditions. To test for the stability of **1a** under the reaction conditions, we kept **1a** in THF at 30 °C for up to 6 days, whereupon we observed 24% decomposition of the diazo compound, which can account for lower total product yields obtained with lower catalyst loadings (vide infra).

Having studied the **1a** → **2a** + **3a** reaction at 0.1 mol% loading of Rh$_2$(esp)$_2$ catalyst, we proceeded to investigate the influence of the catalyst loading (catalyst concentration, *c*) on the **3a/2a** ratio for the same reaction catalyzed by six different Rh(II) catalysts shown in Figure 3. All the reactions were run at 30 °C for 72 h to achieve full conversion even at low catalyst loading, except for the reactions catalyzed by 0.01 mol% of the Rh(II) catalyst, for which the temperature was raised to 50 °C in order to achieve full conversion over the same period of time.
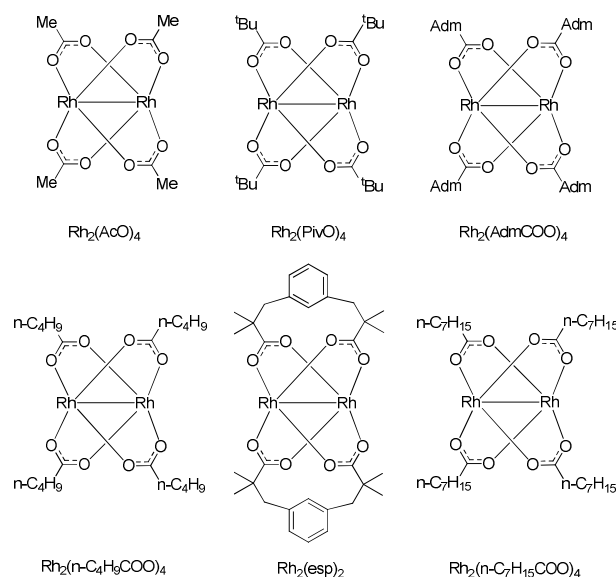

Figure 3. Rh(II) catalysts investigated for the influence of catalyst loading on the product composition.

It was established (see Table S2 in Supplementary Materials) that the catalyst concentration (c_{Rh}) has a strong influence on the chemoselectivity ($S_{3/2} = c_{3a}/c_{2a}$) of the reaction, as seen on the $S_{3/2}$ vs. c_{Rh} and lg$S_{3/2}$ vs. lgC_{Rh} plots (Figure 4).

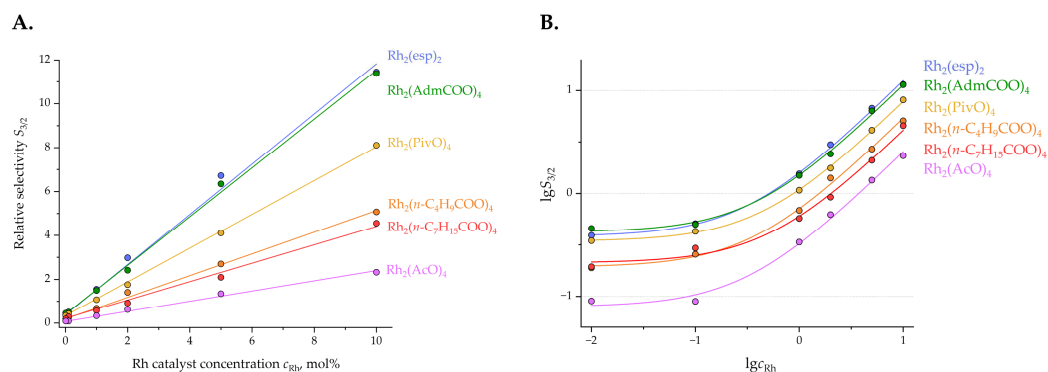**Figure 4.** Chemoselectivity ($S_{3/2} = c_{3a}/c_{2a}$) of **1a** → **2a** + **3a** reaction performed with different catalysts and catalyst loadings: (**A**) in linear coordinates; and (**B**) in logarithmic coordinates.

Examination of the plot presented in Figure 4 reveals that by manipulating the catalyst loading, the chemoselectivity of the **1a** → **2a** + **3a** reaction can be switched from the

preferred formation of spirocyclic product **2a** to the preference for C-H insertion product **3a** (by up to 1.5 orders of magnitude for a given catalyst). Remarkably, rhodium(II) acetate turned out to be particularly suitable for the preparation of spirocycle **2a** at low catalyst concentrations, while rhodium(II) espinoate ($Rh_2(esp)_2$) or adamantanoate ($Rh_2(AdmCOO)_4$) gave a clear preference for the C-H insertion at catalyst concentrations as high as 10 mol%. Notably, these findings proved to be of preparative value, vide infra. Catalyst loading as low as 0.001 mol% was investigated as well and was found to result in no conversion of the starting material.

The apparent switch of the reaction chemoselectivity from product **2a** at low catalyst concentrations to product **3a** at higher (up to 10 mol%) catalyst concentrations can be rationalized from the mechanistic and kinetic perspectives as follows (Scheme 2).
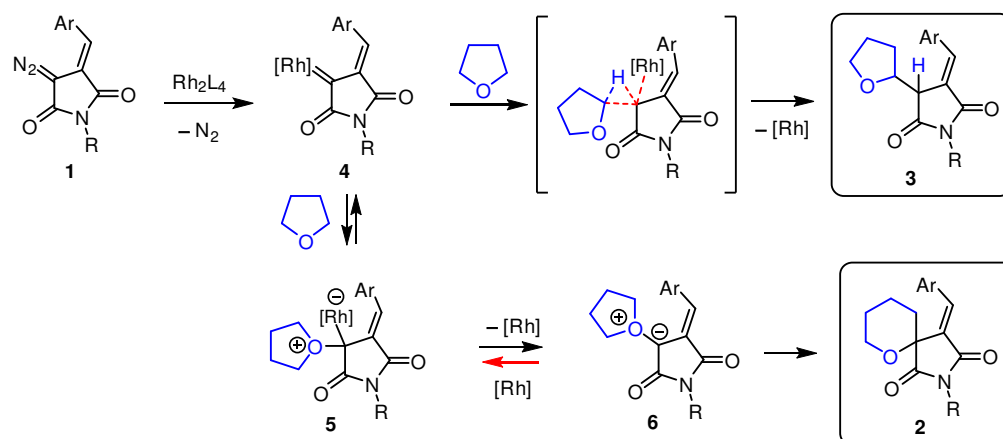
Scheme 2. Plausible mechanistic picture accounting for the formation of compounds **2** and **3**.

Upon the formation of rhodium carbene species **4** (which is a rate-limiting step [13], thereby leaving a significant amount of free catalyst in the reaction mixture), the reaction can proceed in two alternative directions. The C-H insertion to form **3** is likely irreversible. However, the formation of oxonium ylide **6** (preceding the Stevens-type rearrangement to form spirocycle **2**) can be reversible, and these species are in equilibrium with rhodium-containing species **5** and **4**. That means that at higher catalyst loadings (concentrations), this equilibrium will be shifted away from oxonium ylide **6**, and more of the C-H insertion product will be formed. On the contrary, at lower catalyst concentration, the propensity of rhodium carbene **4** to evolve along the pathway leading to spirocycle **2** will be higher.

From the standpoint of kinetics, the said mechanism can be presented as the following scheme (Scheme 3), where k_1–k_4 and k_{-3} are the rate constants for the respective processes.
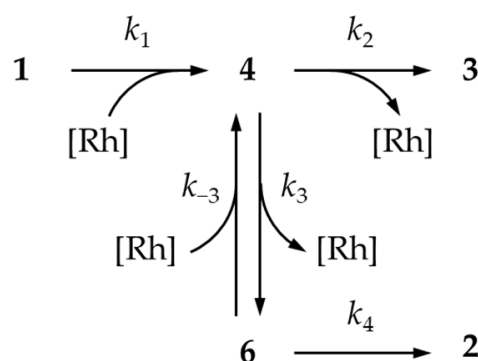
Scheme 3. Schematic representation of the reactions' mechanism for kinetic interpretation.

An important feature of this scheme is the reversibility of the third step, which determines that the ratio of intermediates **4** and **6** depends on the catalyst concentration.

The rates of the formation of products **2** and **3** can be expressed as:

$$\frac{dc_2}{dt} = k_4 c_6 \tag{1}$$

$$\frac{dc_3}{dt} = k_2 c_4 \tag{2}$$

Therefore, the differential selectivity ($s_{3/2}$) of the reaction can be expressed as:

$$s_{3/2} = \frac{dc_3}{dc_2} = \frac{k_2 c_4}{k_4 c_6} \tag{3}$$

Intermediate **6** is highly reactive; therefore, we can apply quasi-stationary approximation:

$$\frac{dc_6}{dt} = k_3 c_4 - k_{-3} c_{\text{Rh}} c_6 - k_4 c_6 \approx 0 \tag{4}$$

Thus, the concentration ratio of intermediates **4** and **6** can be expressed as

$$\frac{c_4}{c_6} = \frac{k_{-3}}{k_3} c_{\text{Rh}} + \frac{k_4}{k_3} \tag{5}$$

and used in the expression for differential selectivity (3) as follows:

$$s_{3/2} = \frac{k_2 k_{-3}}{k_3 k_4} c_{\text{Rh}} + \frac{k_2}{k_3} \tag{6}$$

If we suppose that the catalyst concentration remains unchanged during the course of the reaction and that most of the catalyst remains in the free form, the catalyst concentration (c_{Rh}) equals the catalyst loading. That means that the differential selectivity of the reaction ($s_{3/2}$) does not change with time and equals the integral selectivity $S_{3/2}$:

$$S_{3/2} = \frac{c_3}{c_2} = \frac{k_2 k_{-3}}{k_3 k_4} c_{\text{Rh}} + \frac{k_2}{k_3} \tag{7}$$

The above equation presents the selectivity of the reaction as a linear function of the catalyst concentration, which was observed experimentally (Figure 4A). The components of this linear function ($S = kc + b$) are

$$k = \frac{k_2 k_{-3}}{k_3 k_4} \tag{8}$$

and

$$b = \frac{k_2}{k_3} \tag{9}$$

It was noticed that for the six catalysts under study, a positive linear correlation exists between these parameters (Figure 5).

Considering that the linear function slope (k) can be expressed via its intercept (b)

$$k = \frac{k_{-3}}{k_4} b, \tag{10}$$

we can conclude that the k_{-3}/k_4 ratio only weakly depends on the nature of the catalyst while the k_2/k_3 ratio (or b) depends on the catalyst quite strongly.

Our hypothesis suggests that the variation in the catalyst loading (concentration) determines the likelihood of shifting the equilibrium away from intermediate **6** (and product **2**). In order to further verify this notion, we performed reactions of **1a** in varying volumes of THF with a constant amount of $Rh_2(esp)_2$ catalyst (1 mol%). As expected, simply by increasing the dilution, the selectivity of the reaction shifted from **3a** to **2a** (Table 2).

Table 2. Outcome of **1a** → **2a** + **3a** reaction performed at different dilutions.

THF V (mL)	C (1a), mg/mL	Yield of 2a (%)	Yield of 3a (%)	Fraction of 3a (%)
0.5	60.6	28	72	72
1.0	30.3	38	62	62
3.0	15.2	47	41	47
5.0	7.6	41	25	38
10.0	3.8	56	29	34
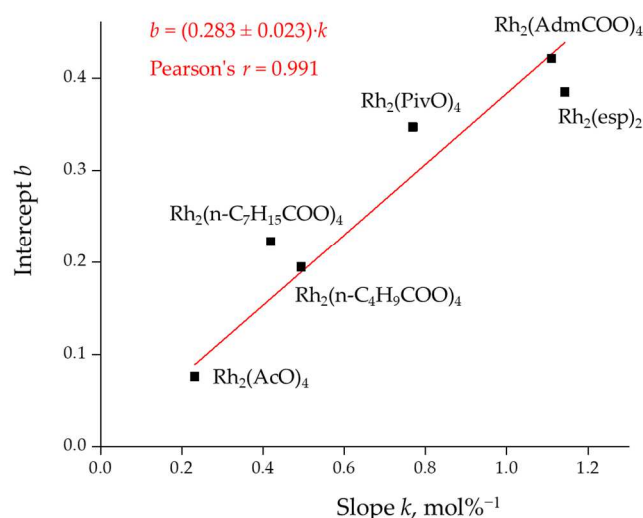
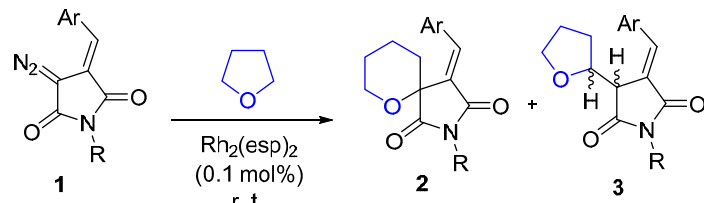**Figure 5.** Linear relationship between parameters k and b for catalysts investigated herein.

Having established the apparent dependence of the course of Rh(II)-catalyzed reaction of diazo compound **1a** with THF on the catalyst loading (concentration), we proceeded to investigate if these findings (gathered by HPLC analysis of reaction mixtures) would translate into sound isolated yields of respective spirocyclic and C-H insertion products for reactions performed on a larger scale. To this end, we selected four DAS substrates **1a–d** described earlier [8] and performed their decomposition by 10 mol% and 0.01 mol% of rhodium(II) acetate as well as rhodium(II) adamantane carboxylate in THF at 30 °C. The isolated yields of products **2(3)a–d** obtained in these reactions are summarized in Table 3.

As can be seen from the data collated in Table 3, the chemoselectivity switch translated very well into the preparation of individual compounds **2** and **3**. A significant switch was achieved with both catalysts employed, depending on the substrate. The highest yield of both products was achieved by changing the catalyst loading by three orders of magnitude for substrate **1b** with both catalysts. However, the chemoselectivity switch from product **2** (with 0.01 mol% of the catalyst) to product **3** (with 10 mol% of the catalyst) was evident and quite significant in all cases studied. It is worthy of note that with large catalyst loadings, the costly rhodium(II) catalysts could be recovered via chromatography and used in subsequent syntheses.

Table 3. Preparative (isolated) yields of products **2** and **3** in the reactions of DAS substrates with THF in the presence of varying Rh(II) catalyst loadings.

Entry	Substrate	Ar	R	Catalyst	mol%	Yield 2 (%)	Yield 3 (%)
1	**1a**	Ph	Bn	$Rh_2(OAc)_4$	10	15	38
2	**1a**	Ph	Bn	$Rh_2(OAc)_4$	0.01	46	7
3	**1a**	Ph	Bn	$Rh_2(AdmO)_4$	10	10	72
4	**1a**	Ph	Bn	$Rh_2(AdmO)_4$	0.01	49	30
5	**1b**	Ph	Ph	$Rh_2(OAc)_4$	10	26	60
6	**1b**	Ph	Ph	$Rh_2(OAc)_4$	0.01	78	20
7	**1b**	Ph	Ph	$Rh_2(AdmO)_4$	10	7	76
8	**1b**	Ph	Ph	$Rh_2(AdmO)_4$	0.01	75	9
9	**1c**	Ph	$4\text{-}FC_6H_4$	$Rh_2(OAc)_4$	10	14	43
10	**1c**	Ph	$4\text{-}FC_6H_4$	$Rh_2(OAc)_4$	0.01	72	4
11	**1d**	$4\text{-}FC_6H_4$	Ph	$Rh_2(OAc)_4$	10	20	66
12	**1d**	$4\text{-}FC_6H_4$	Ph	$Rh_2(OAc)_4$	0.01	69	9

3. Materials and Methods

3.1. General Information

All commercial reagents were used without purification. Tetrahydrofuran was freshly distilled from sodium and benzophenone. NMR spectrum were recorded using Bruker Avance III spectrometer (Billerica, MA, USA) in $CDCl_3$ ([1]H: 400.13 MHz; [13]C: 100.61 MHz; [19]F: 376.50 MHz); NMR spectra are referenced through the solvent lock (2H) signal according to IUPAC recommended secondary referencing method and the manufacturer's protocols; chemical shifts are reported as parts per million (δ, ppm); the residual solvent peak ($CHCl_3$) was used as an internal standard: 7.26 for ^{1}H and 77.16 ppm for ^{13}C; chemical shifts for ^{19}F are given relative to CCl_3F; multiplicities are abbreviated as follows: s = singlet; d = doublet; t = triplet; q = quartet; m = multiplet; br = broad; dd = doublet of doublets; dt = doublet of triplets; ddd = doublet/doublets of doublets; coupling constants, *J*, are reported in Hz. Mass spectra were recorded using Bruker microTOF spectrometer (Münich, Germany) (ionization by electrospray, positive ions detection). Melting points were determined with RD-MP (REACH Devices) melting point apparatus in open capillary tubes. Column chromatography was performed using silica gel Merck (Darmstadt, Germany) grade 60 (0.040–0.063 mm) 230–400 mesh (gradient elution with *n*-hexane−acetone from 19:1 to 1:19). HPLC was performed using the ECS04 Gradient Analytical System instrument and Supelco C_{18} (150 × 3 mm, 5 μm) column at 25 °C eluting with H_2O−MeCN (with addition 0.1% TFA); gradient: 20–30% B (0–5 min), 30–60% B (5–13 min), 60–90% B (13–15 min), and 90% B (15–18 min). Diazo compounds **1a–d** were prepared according to a previously reported method [14].

Performance of **1a** → **2a** + **3a** Reaction on Analytical Scale

To a solution of diazo arylidene succinimide (0.1 mmol) in dry THF in a 2 mL vial, a solution of rhodium catalyst (0.01–10 mol%) in dry THF (dry) was added at 30 °C (or 50 °C for 0.01 mol% catalyst loading) so that the total volume of the solution was 1 mL. The resulting

solution was heated for 72 h in a metal heating block at 30 °C (or 50 °C for 0.01 mol% catalyst loading). Chromatographic analysis was carried out using HPLC; for this, an aliquot of the reaction mixture (0.025 mL) was taken and diluted 40 times with dry THF.

3.2. Reactions of DAS Compounds **1a–d** with THF under Rh(II) Catalysis (Preparative Experiments)

Diazo arylidene succinimide (0.5 mmol) was dissolved in THF (dry) in an 8 mL vial, and a solution of rhodium catalyst (0.01–10 mol%) in THF (dry) was added to the resulting solution at 30 °C (for 10 mol% catalyst loading) or 50 °C (for 0.01 mol% catalyst loading) so that the total volume of the solution was 5 mL. The resulting mixture was stirred for 72 h at 30 °C or 50 °C in a metal heating block. The target products were isolated by chromatography using $5 \to 95\%$ acetone in hexane as eluent.

3.2.1. (*E*)-2-Benzyl-4-benzylidene-6-oxa-2-azaspiro [4.5]decane-1,3-dione (**2a**)

Prepared according to the general procedure for preparative experiments from diazo compound **1a** using $Rh_2(AdmCOO)_4$ (0.01 mol%) as a catalyst. Yield: 85 mg (49%). Colorless viscous oil. Analytical data were in accordance with previously published information [8]. ^{1}H NMR (400 MHz, CDCl$_3$) δ 8.02–7.93 (m, 2H), 7.78 (s, 1H, =CH–), 7.47–7.37 (m, 5H), 7.35–7.19 (m, 3H), 4.77 (s, 2H, N-CH$_2$), 4.61 (ddd, *J* = 13.0, 11.4, 2.6 Hz, 1H), 4.07 (dd, *J* = 11.5, 4.8 Hz, 1H), 2.30 (qt, *J* = 12.7, 4.1 Hz, 1H), 2.13 (td, *J* = 13.8, 4.4 Hz, 1H), 1.85 (dddd, *J* = 17.2, 13.4, 4.4 Hz, 1H), 1.77–1.65 (m, 2H), 1.62–1.48 (m, 1H).

3.2.2. (*E*)-1-Benzyl-3-benzylidene-4-(tetrahydrofuran-2-yl)pyrrolidine-2,5-dione (**3a**)

Prepared according to the general procedure for preparative experiments from diazo compound **1a** using $Rh_2(AdmCOO)_4$ (10 mol%) as a catalyst. Yield: 125 mg (72%). Colorless amorphous solid. Analytical data were in accordance with previously published information [8]. ^{1}H NMR (400 MHz, CDCl$_3$) δ 7.66 (d, *J* = 2.0 Hz, 1H), 7.57–7.46 (m, 2H), 7.48–7.35 (m, 5H), 7.33–7.25 (m, 3H), 4.80 (s, 2H, N-CH$_2$), 4.35–4.23 (m, 1H), 4.02 (t, *J* = 1.7 Hz, 1H), 3.63 (dt, *J* = 8.1, 6.5 Hz, 1H), 3.50 (td, *J* = 7.9, 5.2 Hz, 1H), 2.41 (dq, *J* = 12.3, 8.4 Hz, 1H), 1.98 (dtd, *J* = 12.1, 7.6, 4.2 Hz, 1H), 1.88–1.78 (m, 1H), 1.77–1.63 (m, 1H).

3.2.3. (*E*)-4-Benzylidene-2-phenyl-6-oxa-2-azaspiro [4.5]decane-1,3-dione (**2b**)

Prepared according to the general procedure for preparative experiments from diazo compound **1b** using $Rh_2(AdmCOO)_4$ (0.01 mol%) as a catalyst. Yield: 124 mg (75%). Colorless amorphous solid. Analytical data were in accordance with previously published information [8]. ^{1}H NMR (400 MHz, CDCl$_3$) δ 8.06–8.02 (m, 2H), 7.90 (s, 1H, =CH–), 7.54–7.37 (m, 8H), 4.66 (ddd, *J* = 13.2, 11.4, 2.4 Hz, 1H), 4.14 (dd, *J* = 11.5, 4.8 Hz, 1H), 2.35 (qt, *J* = 11.6, 3.4 Hz, 1H), 2.24 (td, *J* = 13.6, 4.0 Hz, 1H), 1.91 (tddd, *J* = 12.7, 9.5, 6.5, 4.1 Hz, 1H), 1.81–1.67 (m, 3H).

3.2.4. (*E*)-3-Benzylidene-1-phenyl-4-(tetrahydrofuran-2-yl)pyrrolidine-2,5-dione (**3b**)

Prepared according to the general procedure for preparative experiments from diazo compound **1b** using $Rh_2(AdmCOO)_4$ (10 mol%) as a catalyst. Yield: 127 mg (76%). Colorless amorphous solid. Analytical data were in accordance with previously published information [8]. ^{1}H NMR (400 MHz, CDCl$_3$) δ 7.75 (d, *J* = 2.1 Hz, 1H), 7.57–7.54 (m, 2H), 7.52–7.33 (m, 8H), 4.40 (ddd, *J* = 8.5, 7.0, 1.8 Hz, 1H), 4.19 (dd, *J* = 1.9 Hz, 1H), 3.77–3.62 (m, 2H), 2.51 (dq, *J* = 12.4, 8.6 Hz, 1H), 2.10 (dddd, *J* = 12.3, 8.1, 6.9, 4.0 Hz, 1H), 1.95 (dddd, *J* = 14.2, 10.0, 5.8, 2.8 Hz, 1H), 1.87–1.75 (m, 1H).

3.2.5. (*E*)-4-Benzylidene-2-(4-fluorophenyl)-6-oxa-2-azaspiro [4.5]decane-1,3-dione (**2c**)

Prepared according to the general procedure for preparative experiments from diazo compound **1c,** and $Rh_2(AcO)_4$ (0.01 mol%) was used as a catalyst. Yield: 126 mg (72%). Colorless amorphous solid. Analytical data were in accordance with previously published information [8]. ^{1}H NMR (400 MHz, CDCl$_3$) δ 8.07–7.97 (m, 2H), 7.90 (s, 1H, =CH–), 7.49–7.44 (m, 3H), 7.42–7.36 (m, 2H), 7.18 (t, *J* = 8.6 Hz, 2H), 4.64 (ddd, *J* = 13.2, 11.4, 2.6 Hz, 1H), 4.14 (dd, *J* = 11.4, 4.7 Hz, 1H), 2.43–2.16 (m, 2H), 1.96–1.83 (m, 1H), 1.81–1.63 (m, 3H).

3.2.6. (*E*)-3-Benzylidene-1-(4-fluorophenyl)-4-(tetrahydrofuran-2-yl)pyrrolidine-2,5-dione (**3c**)

Prepared according to the general procedure for preparative experiments from diazo compound **1c** using $Rh_2(AcO)_4$ (10 mol%) as a catalyst. Yield: 76 mg (43%). Colorless amorphous solid. Analytical data were in accordance with previously published information [8]. ^{1}H NMR (400 MHz, $CDCl_3$) δ 7.76 (d, *J* = 1.8 Hz, 1H), 7.61–7.52 (m, 2H), 7.49–7.32 (m, 5H), 7.21–7.13 (m, 2H), 4.38 (ddd, *J* = 8.5, 6.9, 1.6 Hz, 1H), 4.18 (t, *J* = 1.9 Hz, 1H), 3.86–3.63 (m, 2H), 2.51 (dq, *J* = 12.3, 8.6 Hz, 1H), 2.10 (dtd, *J* = 12.0, 7.6, 4.0 Hz, 1H), 2.02–1.74 (m, 1H).

3.2.7. (*E*)-4-(4-Fluorobenzylidene)-2-phenyl-6-oxa-2-azaspiro [4.5]decane-1,3-dione (**2d**)

Prepared according to the general procedure for preparative experiments from diazo compound **1d** using $Rh_2(AcO)_4$ (0.01 mol%) as a catalyst. Yield: 121 mg (69%). Colorless amorphous solid. Analytical data were in accordance with previously published information [8]. ^{1}H NMR (400 MHz, $CDCl_3$) δ 8.08–8.03 (m, 2H), 7.84 (s, 1H, =CH–), 7.53–7.47 (m, 2H), 7.44–7.37 (m, 3H), 7.19–7.12 (m, 2H), 4.71–4.63 (m, 1H), 4.12 (dd, *J* = 11.4, 4.7 Hz, 1H), 2.35 (qt, *J* = 12.4, 4.2 Hz, 1H), 2.19 (td, *J* = 13.8, 13.3, 4.3 Hz, 1H), 1.95–1.68 (m, 4H).

3.2.8. (*E*)-3-(4-Fluorobenzylidene)-1-phenyl-4-(tetrahydrofuran-2-yl)pyrrolidine-2,5-dione (**3d**)

Prepared according to the general procedure for preparative experiments from diazo compound **1d** using $Rh_2(AcO)_4$ (10 mol%) as a catalyst. Yield: 116 mg (66%). Colorless amorphous solid. M.p. 181–182 °C. ^{1}H NMR (500 MHz, $CDCl_3$) δ 7.74–7.70 (m, 1H), 7.62–7.54 (m, 2H), 7.52–7.46 (m, 2H), 7.43–7.33 (m, 3H), 7.18–7.11 (m, 2H), 4.39 (dtd, *J* = 8.6, 4.3, 1.7 Hz, 1H), 4.16 (t, *J* = 2.0 Hz, 1H), 3.83 (dt, *J* = 8.4, 6.9 Hz, 1H), 3.76–3.64 (m, 1H), 2.46 (dq, *J* = 12.4, 8.6 Hz, 1H), 2.09 (dddd, *J* = 12.3, 8.1, 7.0, 4.1 Hz, 1H), 2.02–1.74 (m, 2H). ^{13}C NMR (126 MHz, $CDCl_3$) δ 174.5, 170.1, 163.7 (d, *J* = 252.9 Hz), 135.2, 132.6 (d, *J* = 8.2 Hz), 130.3 (d, *J* = 3.4 Hz), 129.3, 128.7, 127.4, 126.7, 125.7, 116.5 (d, *J* = 21.9 Hz), 78.9, 69.2, 48.1, 28.9, 26.1. ^{19}F NMR (470 MHz, $CDCl_3$) δ −108.61. HRMS (ESI), *m/z* calcd for $C_{21}H_{18}FNNaO_3$ [M + Na]$^+$ 374.1163 found 374.1155.

4. Conclusions

We have investigated an unusual and hitherto undescribed phenomenon of chemoselectivity switch from one of the two principal reaction products to the other in the Rh(II)-catalyzed reactions of α-diazo succinimides or DAS with tetrahydrofuran (employed as a solvent). Higher catalyst loading (up to 10 mol%) has been shown to favor the formation of the product resulting from the insertion into α-C-H bond of THF while lowering the catalyst loading by three orders of magnitude (down to 0.01 mol%) led to the predominant formation of spirocyclic product through the intermediacy of oxonium ylide species and Stevens-type rearrangement of the latter. Our mechanistic hypothesis stipulating the reversibility of the oxonium ylide formation rationalizes the observed chemoselectivity switch. It is in agreement with the changes in the product mixture composition observed on simple dilution (i.e., lowering the concentration of all components, including the catalyst). The reversibility of the steps preceding the formation of the spirocyclic product explains the higher proportion of the alternative C-H insertion product obtained with higher catalyst loadings. These findings signify the importance of catalyst loading as the reaction parameter influencing the ratio of alternative reaction products in the reactions of α-diazocarbonyl compounds proceeding via the formation of metal carbene species and following competing pathways. This phenomenon—discovered for the reaction of DAS substrates with THF on Rh(II) catalysis—is likely to be relevant in other metal-catalyzed reactions of α-diazocarbonyl compounds and should be taken into account when optimizing such reactions toward a specific product.

Supplementary Materials: The following supporting information can be downloaded at: https://www.mdpi.com/article/10.3390/catal13020428/s1, Table S1: Results of calibration measurements; Figure S1: Calibration curve for **1a**; Figure S2: Calibration curve for **3a**; Figure S3: Calibration curve for **2a**; Figure S4: HPLC chromatogram of reaction **1a** → **2a** + **3a** after 2 min; Figure S5: HPLC chromatogram of reaction **1a** → **2a** + **3a** after 15 min; Figure S6: HPLC chromatogram of reaction **1a** → **2a** + **3a** after 30 min; Figure S7: HPLC chromatogram of reaction **1a** → **2a** + **3a** after 45 min; Figure S8: HPLC chromatogram of reaction **1a** → **2a** + **3a** after 60 min; Figure S9: HPLC chromatogram of reaction **1a** → **2a** + **3a** after 90 min; Figure S10: HPLC chromatogram of reaction **1a** → **2a** + **3a** after 120 min; Figure S11: HPLC chromatogram of reaction **1a** → **2a** + **3a** after 150 min; Figure S12: HPLC chromatogram of reaction **1a** → **2a** + **3a** after 180 min; Figure S13: HPLC chromatogram of reaction **1a** → **2a** + **3a** after 240 min; Figure S14: HPLC chromatogram of reaction **1a** → **2a** + **3a** after 300 min; Figure S15: HPLC chromatogram of reaction **1a** → **2a** + **3a** after 360 min; Table S2: Outcome of **1a** → **2a** + **3a** reactions performed with different catalysts and catalyst loadings; Figure S16: HPLC chromatogram of **1a** → **2a** + **3a** reaction performed with $Rh_2(AdmCOO)_4$ (0.01 mol%); Figure S17: HPLC chromatogram of **1a** → **2a** + **3a** reaction performed with $Rh_2(AdmCOO)_4$ (0.1 mol%); Figure S18: HPLC chromatogram of **1a** → **2a** + **3a** reaction performed with $Rh_2(AdmCOO)_4$ (1.0 mol%); Figure S19: HPLC chromatogram of **1a** → **2a** + **3a** reaction performed with $Rh_2(AdmCOO)_4$ (2.0 mol%); Figure S20: HPLC chromatogram of **1a** → **2a** + **3a** reaction performed with $Rh_2(AdmCOO)_4$ (5.0 mol%); Figure S21: HPLC chromatogram of **1a** → **2a** + **3a** reaction performed with $Rh_2(AdmCOO)_4$ (10.0 mol%); Figure S22: HPLC chromatogram of **1a** → **2a** + **3a** reaction performed with $Rh_2(PivO)_4$ (0.01 mol%); Figure S23: HPLC chromatogram of **1a** → **2a** + **3a** reaction performed with $Rh_2(PivO)_4$ (0.1 mol%); Figure S24: HPLC chromatogram of **1a** → **2a** + **3a** reaction performed with $Rh_2(PivO)_4$ (1.0 mol%); Figure S25: HPLC chromatogram of **1a** → **2a** + **3a** reaction performed with $Rh_2(PivO)_4$ (2.0 mol%); Figure S26: HPLC chromatogram of **1a** → **2a** + **3a** reaction performed with $Rh_2(PivO)_4$ (5.0 mol%); Figure S27: HPLC chromatogram of **1a** → **2a** + **3a** reaction performed with $Rh_2(PivO)_4$ (10.0 mol%); Figure S28: HPLC chromatogram of **1a** → **2a** + **3a** reaction performed with $Rh_2(esp)_2$ (0.01 mol%); Figure S29: HPLC chromatogram of **1a** → **2a** + **3a** reaction performed with $Rh_2(esp)_2$ (0.1 mol%); Figure S30: HPLC chromatogram of **1a** → **2a** + **3a** reaction performed with $Rh_2(esp)_2$ (1.0 mol%); Figure S31: HPLC chromatogram of **1a** → **2a** + **3a** reaction performed with $Rh_2(esp)_2$ (2.0 mol%); Figure S32: HPLC chromatogram of **1a** → **2a** + **3a** reaction performed with $Rh_2(esp)_2$ (5.0 mol%); Figure S33: HPLC chromatogram of **1a** → **2a** + **3a** reaction performed with $Rh_2(esp)_2$ (10.0 mol%); Figure S34: HPLC chromatogram of **1a** → **2a** + **3a** reaction performed with $Rh_2(AcO)_4$ (0.01 mol%); Figure S35: HPLC chromatogram of **1a** → **2a** + **3a** reaction performed with $Rh_2(AcO)_4$ (0.1 mol%); Figure S36: HPLC chromatogram of **1a** → **2a** + **3a** reaction performed with $Rh_2(AcO)_4$ (1.0 mol%); Figure S37: HPLC chromatogram of **1a** → **2a** + **3a** reaction performed with $Rh_2(AcO)_4$ (2.0 mol%); Figure S38: HPLC chromatogram of **1a** → **2a** + **3a** reaction performed with $Rh_2(AcO)_4$ (5.0 mol%); Figure S39: HPLC chromatogram of **1a** → **2a** + **3a** reaction performed with $Rh_2(AcO)_4$ (10.0 mol%); Figure S40: HPLC chromatogram of **1a** → **2a** + **3a** reaction performed with $Rh_2(n\text{-}C_4H_9COO)_4$ (0.01 mol%); Figure S41: HPLC chromatogram of **1a** → **2a** + **3a** reaction performed with $Rh_2(n\text{-}C_4H_9COO)_4$ (0.1 mol%); Figure S42: HPLC chromatogram of **1a** → **2a** + **3a** reaction performed with $Rh_2(n\text{-}C_4H_9COO)_4$ (1.0 mol%); Figure S43: HPLC chromatogram of **1a** → **2a** + **3a** reaction performed with $Rh_2(n\text{-}C_4H_9COO)_4$ (2.0 mol%); Figure S44: HPLC chromatogram of **1a** → **2a** + **3a** reaction performed with $Rh_2(n\text{-}C_4H_9COO)_4$ (5.0 mol%); Figure S45: HPLC chromatogram of **1a** → **2a** + **3a** reaction performed with $Rh_2(n\text{-}C_4H_9COO)_4$ (10.0 mol%); Figure S46: HPLC chromatogram of **1a** → **2a** + **3a** reaction performed with $Rh_2(n\text{-}C_7H_{15}COO)_4$ (0.01 mol%); Figure S47: HPLC chromatogram of **1a** → **2a** + **3a** reaction performed with $Rh_2(n\text{-}C_7H_{15}COO)_4$ (0.1 mol%); Figure S48: HPLC chromatogram of **1a** → **2a** + **3a** reaction performed with $Rh_2(n\text{-}C_7H_{15}COO)_4$ (1.0 mol%); Figure S49: HPLC chromatogram of **1a** → **2a** + **3a** reaction performed with $Rh_2(n\text{-}C_7H_{15}COO)_4$ (2.0 mol%); Figure S50: HPLC chromatogram of **1a** → **2a** + **3a** reaction performed with $Rh_2(n\text{-}C_7H_{15}COO)_4$ (5.0 mol%); Figure S51: HPLC chromatogram of **1a** → **2a** + **3a** reaction performed with $Rh_2(n\text{-}C_7H_{15}COO)_4$ (10.0 mol%); Figure S52: HPLC chromatogram of the reaction **1a** → **2a** + **3a** in 0.5 mL of THF; Figure S53: HPLC chromatogram of the reaction **1a** → **2a** + **3a** in 1 mL of THF; Figure S54: HPLC chromatogram of the reaction **1a** → **2a** + **3a** in 3 mL of THF; Figure S55: HPLC chromatogram of the reaction **1a** → **2a** + **3a** in 5 mL of THF; Figure S56: HPLC chromatogram of the reaction **1a** → **2a** + **3a** in 10 mL of THF. Key HPLC chromatograms, calibration curves for the model set of starting materials and

products, experimental results with catalyst and catalyst loading variations, and copies of NMR spectra for compounds **2a–d** and **3a–d**.

Author Contributions: A.K.: investigation (performance of all chemistry experiments); I.A.R.: investigation and methodology (interpretation and analysis of the experimental kinetics data); O.B.: investigation, methodology (chromatography experiments); G.K.: investigation (starting material synthesis); D.D.: supervision, methodology; M.K.: supervision, funding acquisition, manuscript writing. All authors have read and agreed to the published version of the manuscript.

Institutional Review Board Statement: Not applicable.

Informed Consent Statement: Not applicable.

Data Availability Statement: Not applicable.

Conflicts of Interest: The authors declare no conflict of interest.

References

1. Ye, T.; McKervey, M.A. Organic Synthesis with alpha-Diazo Carbonyl Compounds. *Chem. Rev.* **1994**, *94*, 1091–1160.
2. Chupakhin, E.; Gecht, M.; Ivanov, A.; Kantin, G.; Dar'in, D.; Krasavin, M. (*E*)-3-Arylidene-4-diazopyrrolidine-2,5-diones: Preparation and use in Rh^{II}-catalyzed X–H insertion reactions towards novel, medicinally important Michael acceptors. *Synthesis* **2021**, *53*, 1292–1300.
3. Doyle, M.P.; Duffy, R.; Ratnikov, M.; Zhou, L. Catalytic Carbene Insertion into C−H Bonds. *Chem. Rev.* **2010**, *110*, 704–724.
4. Guranova, N.I.; Dar'in, D.; Kantin, G.; Novikov, A.S.; Bakulina, O.; Krasavin, M. Rh(II)-Catalyzed Spirocyclization of α-Diazo Homophthalimides with Cyclic Ethers. *J. Org. Chem.* **2019**, *84*, 4534–4542.
5. Wang, H.; Guptill, D.M.; Alvarez, A.V.; Musaev, D.G.; Davies, H.M.L. Rhodium-catalyzed enantioselective cyclopropanation of electron deficient alkenes. *Chem. Sci.* **2013**, *4*, 2844–2850.
6. Laha, D.; Bhat, R.G. Silver-Catalyzed Epoxidation of Aldehydes Using Donor-/Acceptor-type Vinyl Diazosuccinimides to Access Spiro Pyrrolidinedione Oxiranes. *Asian J. Org. Chem.* **2020**, *9*, 918–921.
7. Budeev, A.; Kantin, G.; Dar'in, D.; Krasavin, M. Diazocarbonyl and Related Compounds in the Synthesis of Azoles. *Molecules* **2021**, *26*, 2530.
8. Dar'in, D.; Kantin, G.; Bakulina, O.; Inyutina, A.; Chupakhin, E.; Krasavin, M. Spirocyclizations involving oxonium ylides derived from cyclic α-diazocarbonyl compounds: An entry into 6-oxa-2-azaspiro [4.5]decane scaffold. *J. Org. Chem.* **2020**, *85*, 15586–15599.
9. Inyutina, A.; Dar'in, D.; Kantin, G.; Krasavin, M. Tricyclic 2-Benzazepines Obtained via an Unexpected Cyclization Involving Nitrilium Ylides. *Org. Biomol. Chem.* **2021**, *19*, 5068–5071.
10. Inyutina, A.; Kantin, G.; Dar'in, D.; Krasavin, M. Diastereoselective Formal [5+2] Cycloaddition of Diazo Arylidene Succinimides-Derived Rhodium Carbenes and Aldehydes: A Route to 2-Benzoxepines. *J. Org. Chem.* **2021**, *86*, 13673–13683.
11. Vepreva, A.; Kantin, G.; Krasavin, M.; Dar'in, D. A General Way to Spiro-Annulated 2-Benzoxepines via Rh2(esp)2-catalyzed [5+2] Cycloaddition of Diazo Arylidene Succinimides to Ketones. *Synthesis* **2022**, *54*, 5128–5138.
12. Vepreva, A.; Bunev, A.S.; Kudinov, A.Y.; Kantin, G.; Krasavin, M.; Dar'in, D. Unusual Highly Diastereoselective Rh(II)-catalyzed Dimerization of Diazo Arylidene Succinimides Provides Access to New Dibenzazulene Scaffold. *Beilstein J. Org. Chem.* **2022**, *18*, 533–538.
13. Nakamura, E.; Yoshikai, N.; Yamanaka, M. Mechanism of C−H Bond Activation/C−C Bond Formation Reaction between Diazo Compound and Alkane Catalyzed by Dirhodium Tetracarboxylate. *J. Am. Chem. Soc.* **2002**, *124*, 7181–7192.
14. Chupakhin, E.G.; Kantin, G.P.; Dar'in, D.V.; Krasavin, M. Convenient preparation of (*E*)-3-arylidene-4-diazopyrrolidine-2,5-diones in array format. *Mendeleev Commun.* **2021**, *31*, 36–38.